Preprint | https://doi.org/10.64560/65530516

AGILOped: Agile Open-Source Humanoid Robot for Research

Grzegorz Ficht
ficht@ais.uni-bonn.de
University of Bonn

Luis Denninger
denninger@ais.uni-bonn.de
University of Bonn

Sven Behnke
behnke@ais.uni-bonn.de
University of Bonn

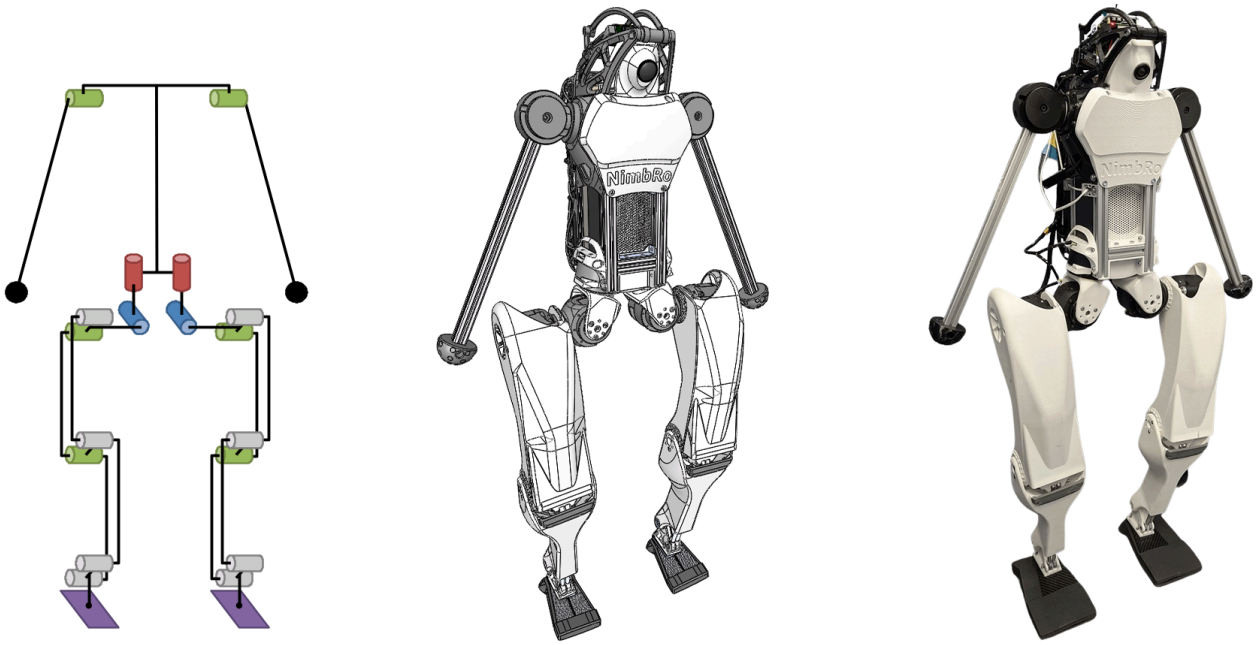

Abstract: With academic and commercial interest for humanoid robots peaking, multiple platforms are being developed. Through a high level of customization, they showcase impressive performance. Most of these systems remain closed-source or have high acquisition and maintenance costs, however. In this work, we present AGILOped - an open-source humanoid robot that closes the gap between high performance and accessibility. Our robot is driven by off-the-shelf backdrivable actuators with high power density and uses standard electronic components. With a height of 110 cm and weighing only 14.5 kg, AGILOped can be operated without a gantry by a single person. Experiments in walking, jumping, impact mitigation and getting-up demonstrate its viability for use in research.

Tags: Robotics, Open-source

1 Introduction

Humanoid robotics is currently experiencing a surge in development, fueled by the elusive idea of universal automatons capable of performing work at a level similar to humans. This is the result of several key technologies maturing to the point of viability. Energy-dense and compact batteries and efficient motor controllers are able to quickly provide sufficient power to actuators, enabling powerful and dynamic motions.The miniaturization of computing has enabled the embedding of online controls based on complex dynamics, as well as the use of Large Language Models. These have the ability to perform unstructured, unfamiliar tasks using multimodal input, evoking the sense of human reasoning.

Preprint | https://doi.org/10.64560/65530516

Developing and integrating all these capabilities into a single platform is not trivial.The needed multidisciplinary knowledge requires the collaboration of highly skilled professionals working in a dedicated, specialized environment. This comes at a cost, leaving development to a small number of players with the resources to sustain it. Such exclusivity of a universally applicable technology can have far-reaching socio-economic consequences, highlighting the need for accessible and open solutions.

With **AGILOped**, shown in Teaser Figure, we introduce a dynamically capable, open and affordable research platform. By relying only on a 3D printer, off-the-shelf components and basic tooling, we greatly lower the entry barrier to humanoid robotics research. We describe the design principles, our hardware choices, and present results showcasing the robot's capabilities.

2 Related Work

Creating bipedal robots, able to reproduce the dynamic motions of humans has been a long-standing research interest. The MIT 3D Biped*(Playter & Raibert, 1992)* was the first successful example capable of performing both untethered running and somersaults, a feat which hasn't been reproduced by a biped for the next 25 years*(Boston Dynamics, 2017)*. Running was also achieved by ATRIAS*(Hubicki et al., 2016)* with speeds exceeding 9km/h. Both robots are embodiments of the Spring-Loaded Inverted Pendulum (SLIP) model. Their hip-concentrated mass and low-inertia legs allow to achieve explosive dynamic motions without need for complex controls, demonstrating the strength of a SLIP hardware template.

Performing such dynamic motions requires actuators not only capable of producing the necessary peak power, but also capable of sustaining the repetitive high impact forces. While the hydraulics used in Atlas offer extreme forces and naturally absorb impacts, they are the least user-friendly to work with due to noise and possible leakages. Furthermore, hydraulic actuators are not energy-efficient. Series-Elastic Actuators (SEAs) are an alternative, as the embedded spring allows for energy storage and control through the relationship between force and displacement*(Negrello et al., 2015)*. The spring limits the possible control bandwidth, though. Recent Quasi Direct Drive (QDD) actuators with Brushless DC motors and integrated planetary gearbox do not suffer from this limitation. Originally developed for the Mini-Cheetah*(Katz et al., 2019)*, they have been successfully applied to several recent humanoid designs*(@sim2022tello, @li2023dynamic, @artemis2023, @saloutos2023design, Liao et al., 2024)*.

Having resilient actuators might not always be sufficient to prevent hardware damage. As bipeds inevitably do fall, implementing various falling strategies is a viable option *(@Qingqing2017fall, @Ogata2007fall, @goswami2014fall, Kakiuchi et al., 2017)*. These strategies generally focus on damping the fall using the arms and bending the knees to reduce the fall height, as humans would. However, further design-related approaches, such as those explored by Wilken et al. *(Wilken et al., 2009)*, who designed compliant arms, have unfortunately been widely understudied. While recent robots have demonstrated improved dynamic motion capabilities, their ability to withstand repeated falls remains largely unexplored. A biomimetic approach of enveloping a rigid structure

Preprint | https://doi.org/10.64560/65530516

with materials imitating soft tissues, might prove to be beneficial for reducing damage sustained from falling.

Table 1: Comparison of established and recently developed humanoid platforms.

Platform	Height (cm)	Weight (kg)	Price (USD)	Materials (main)	Open Source (CAD)	Off-the-shelf	Max. HFE[c] Tor. (Nm)	Max. KFE[d] Tor. (Nm)
NAO [11]	57	4.5	14K	Plastic	Yes	No	1.61[b]	1.61[b]
DARwIn-OP [12]	45	2.8	12K	Plastic	Yes	Yes	2.35[b]	2.35[b]
Booster T1 [13][14]	120	30	34K	Metal	No	No	-	130
NimbRo-OP2x [15]	135	19	25K	Plastic	Yes	Yes	40[a,b]	80[a,b]
Unitree H1 [16]	130	35	90K	Metal	No	No	88	139
MIT Humanoid [17]	70	21	-	Metal	No	No	72	144
ARTEMIS [8]	142	37	-	Metal	No	No	250	250
Unitree G1 [16][14]	130	35	16K[e]-35K[f]	Metal	No	No	88	139
Fourier GR-1 [18][14]	165	60	200K	Metal	No	No	230	230
Berkeley Humanoid [10]	85	22	10K	Metal	No	No	62.6	81.1
AGILOped (ours)	110	14.5	6.5K	Plastic	Yes	Yes	40[a]	80[a]

[a]joint-configuration-dependent [b]stall [c]hip flexion/extension [d]knee flexion/extension [e]non-programmable [f]for developers

While it has been shown that humanoid platforms can achieve human-like dynamic motions, most remain inaccessible to many research groups. Table 1 provides an overview of recently developed platforms. The platforms cited above, coming from research groups, such as the MIT Humanoid *(SaLoutos et al., 2023)*, Berkeley Humanoid *(Liao et al., 2024)*, HECTOR*(Li et al., 2023)* and ARTEMIS *(Zhu, 2023)*, are unavailable to those interested. Because they use custom components, their results are not reproducible by other researchers. Although commercially available humanoids are on the horizon, e.g. Unitree G1 *(Unitree Robotics, 2024)*, Fourier-GR1 *(Fourier Intelligence, 2024)*, and Booster T1 *(Booster Robotics, 2024)*, they come with their drawbacks. They are either expensive, make the user dependent on the manufacturer, or come with limited source-code access. This typically restricts full control, particularly at the low level, making these platforms less attractive for research purposes.

Alternatively, the NimbRo-OP2X *(Ficht et al., 2020)* platform or iterations of the DARwIn-OP *(Ha et al., 2011)* offer a more research-friendly solution. These systems provide access to freely available CAD models and utilize off-the-shelf actuators, allowing for full control over hardware and simplifying maintenance. However, their limited motor specifications or small size prevent them from achieving the dynamic motions of modern humanoids, highlighting the need for a dynamic and accessible platform.

3 Design

The design of our robot is intended to provide a low entry point into humanoid robotics development without compromising on the ability to perform dynamic tasks. To achieve this, the platform must be universally accessible, which includes obtaining the robot at an affordable price, effortless and reliable operation, easy maintenance, and customization possibilities. An overview of the hardware specifications of **AGILOped**, is given in Table 2. With a height of 110cm and weight of 14.5kg, it matches the measurements of a typical 6-year-old child. The size was intentionally chosen for its balance of meaningful interaction and safe operation within human-scale environments. We leverage our experience with 3D-printed humanoids *(@ficht2017nop2, Ficht et*

Preprint | https://doi.org/10.64560/65530516

al., 2020) to make **AGILOped**, accessible and easily manufactured using only a commercially available 3D printer and basic tools. This enables modularity, as parts can quickly be altered to have improved physical properties, house newer components or implement novel functionality. The design heavily relies on selective compliance, efficiently combining the rigidity of aluminum and flexibility of 3D-printed plastics and polyurethanes of varying hardness to deliver cohesive, minimalistic and robust robot hardware.

For the design of **AGILOped**, we utilized off-the-shelf components to significantly simplify manufacturing and maintenance. Off-the-shelf items are cost-effectively produced at scale, extensively tested by the manufacturer, well-documented and ready to use. With only 10 actuators controlling 12 joints, we emphasize simplicity and cost-effectiveness assuring that the robot is approachable to users with varying levels of experience. Through careful selection of modular components and materials embedded in a light-weight design, we have achieved a price point of 6,380 USD, making **AGILOped** the most affordable and lightest humanoid in its size class. To promote collaboration and reduce exclusivity within the field of humanoid robotics, the design files were open-sourced online.

Table 2: **AGILOped**, specifications.

Type	Specification	Value
General	Height & Weight	110 cm, 14.5 kg
	Battery	2×LiPo (26.1 V, 4.5 Ah)
	Battery life	1.5–2.5 h
	Material	Aluminum, PLA/Nylon, TPU
Computing	Base Controller	RaspBerry Pi 3B+
	Specs	4×1.4 GHz, 1 GB RAM
	I/O	4×USB 2.0, GPIOs, 1×HDMI, Ethernet, Wi-Fi
	(Optional)	NVIDIA Jetson
Actuators	Total	10 × MyActuator RMD X6-40
	Torque	18 Nm (Rated), 40 Nm (Peak)
	No load speed (48V)	11.5 rad/s
	Feedback	Position, Velocity, Torque
	Encoder (Motor)	16 bit/rev
	Communication	CAN (1Mbit)
Cost (USD)	Actuators	10 × 545
	Batteries	2 × 150
	IMU	1 × 30
	Raspberry Pi 3B+	1 × 35
	PiCAN2Duo	1 × 70
	Misc Hardware	1 × 495
	NVidia Jetson	1 × (200 – 2000)
	Total	6,380 (6,580 – 8,380)

3.1 Actuator Module and Power

Originally custom-developed as a novel actuator for the Mini-Cheetah *(Katz et al., 2019)*, Quasi Direct Drives (QDD) with brushless DC motors and integrated planetary transmission offer high torque density and control at high bandwidths. Through in-house development one might have more control over aspects of the design process, but it is associated with significant costs in time and effort through development, testing and manufacturing. Derivatives of these actuators have

since become widely used in legged robotics and available from numerous vendors in various sizes*(@tmotor, @westwood, MyActuator, 2024)*. We opt to use the MyActuator RMD X6-40 with *two-stage* planetary gearing for all joints, mainly for its high torque within a compact, modular form-factor see Table 2.

Because of the direct correlation of motor diameter and torque, it may seem counter-intuitive to opt for a low-diameter motor. The X6-40 compensates for this by a 1:36 planetary gearbox, provide up to 40Nm torque. This is not detrimental to proprioception, due to the smaller radius keeping the rotor inertia low 28.8kg,cm^2. It is lower than that of a large-diameter, flat X10-40 actuator (39.7kg,cm^2), with single-stage 1:7 planetary gearbox and similar peak torques of 40Nm, but twice the weight (1.1kg)*(MyActuator, 2024)*.

Despite the extra reduction stage, X6-40 can reach angular velocities exceeding 10rad/s, which is equivalent to peak joint velocities of a human sprinting faster than 6m/s *(Belli et al., 2002)*. For the same output speed, the motor turns faster---compared to actuators with lower gear ratio---which improves motor efficiency and, thus, reduces thermal load. Although actuators in a similar weight class are capable of providing higher no-load speeds~(e.g. Unitree A1), their cost is roughly double that of the X6-40, while providing only 80% of its peak torque. Each X6-40 actuator has an integrated motor controller, equipped with a high-resolution 16-bit encoder mounted on the motor shaft. The chosen actuators operate with voltages in the range 20--52V in position, velocity, torque and impedance control mode. Commands and feedback are transmitted over a CAN bus.

To operate the actuators at the maximum possible velocity, we use two 26.1V UAV batteries connected in series for a total supply voltage of 52.2V. The high-power density, protection features, rugged casing, smart switch and charge manager remove the necessity to design specialized electronics around raw cells. We take advantage of this by implementing a hot-swap circuit based on two high-power diodes (as seen in Figure 4). In normal operation, the diodes are reverse-biased and the batteries are directly connected to the motors. When any of the batteries is removed for a swap, the diode closes the circuit. The simplicity and cost-effectiveness of this setup comes with the requirement that all components need to tolerate a wide voltage input.

3.2 Leg Design

Each leg features a hybrid, serial-parallel kinematic chain with five joints and biologically inspired elements. The leg joints are powered through four collocated actuators: three at the hip (yaw, roll, pitch) and one at the knee~(pitch). All axes in the hip intersect at a common point to simplify the kinematics. The outward hip pitch placement aims to mimic the bicondylar angle of the femoral shaft naturally acquired by humans, which is known to increase their efficiency. This is due to a part of the load being distributed to the skeletal structure, but also by allowing the feet to be placed closer to the midline---minimizing lateral movement *(@bramble2004endurance, @tayton2007femoral, Tardieu, 2010)*. In the sagittal plane, we employ double 4-bar parallelograms (actuated at the q_{th} thigh and q_{sh} shank) that control the hip q_h, knee q_k and ankle q_a:

Preprint | https://doi.org/10.64560/65530516

$$q_h = q_{th}, \quad q_k = q_{sh} - q_{th}, \quad q_a = -q_{sh} \tag{1}$$

First, this reduces the number of actuators~(thus the inertia) and achieves a completely passive ankle joint q_a with the foot orientation horizontally constrained to the torso. The second benefit is a faster knee, and torque τ_k shared between thigh and shank. This is defined by the mapping Jacobian **J**, obtained through differentiating Equation 1:

$$\begin{bmatrix} \dot{q}_h \\ \dot{q}_k \\ \dot{q}_a \end{bmatrix} = \mathbf{J} \begin{bmatrix} \dot{q}_{th} \\ \dot{q}_{sh} \end{bmatrix}, \quad \begin{bmatrix} \tau_h \\ \tau_k \\ \tau_a \end{bmatrix} = \mathbf{J} \begin{bmatrix} \tau_{th} \\ \tau_{sh} \end{bmatrix}, \quad \mathbf{J} = \begin{bmatrix} 1 & 0 \\ -1 & 1 \\ 0 & -1 \end{bmatrix}. \tag{2}$$

The parallelograms are neatly hidden within the 3D-printed structure, and despite their presence we are able to achieve a high range of motion Figure 2.

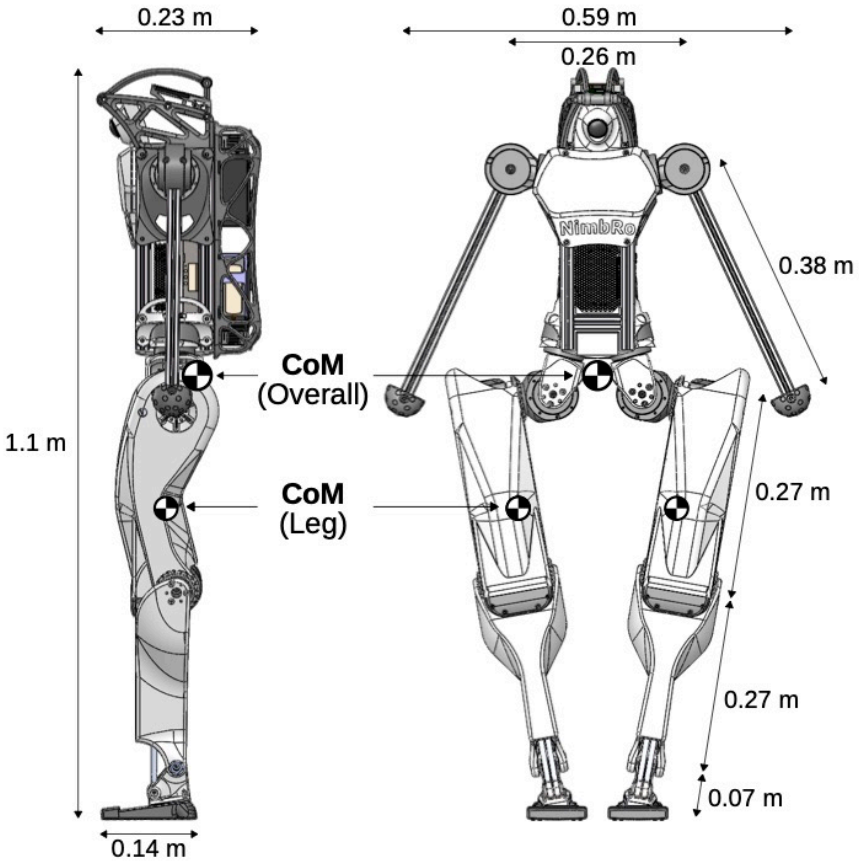

Figure 1: **AGILOped**dimensions labelled in frontal and side view.

Preprint | https://doi.org/10.64560/65530516

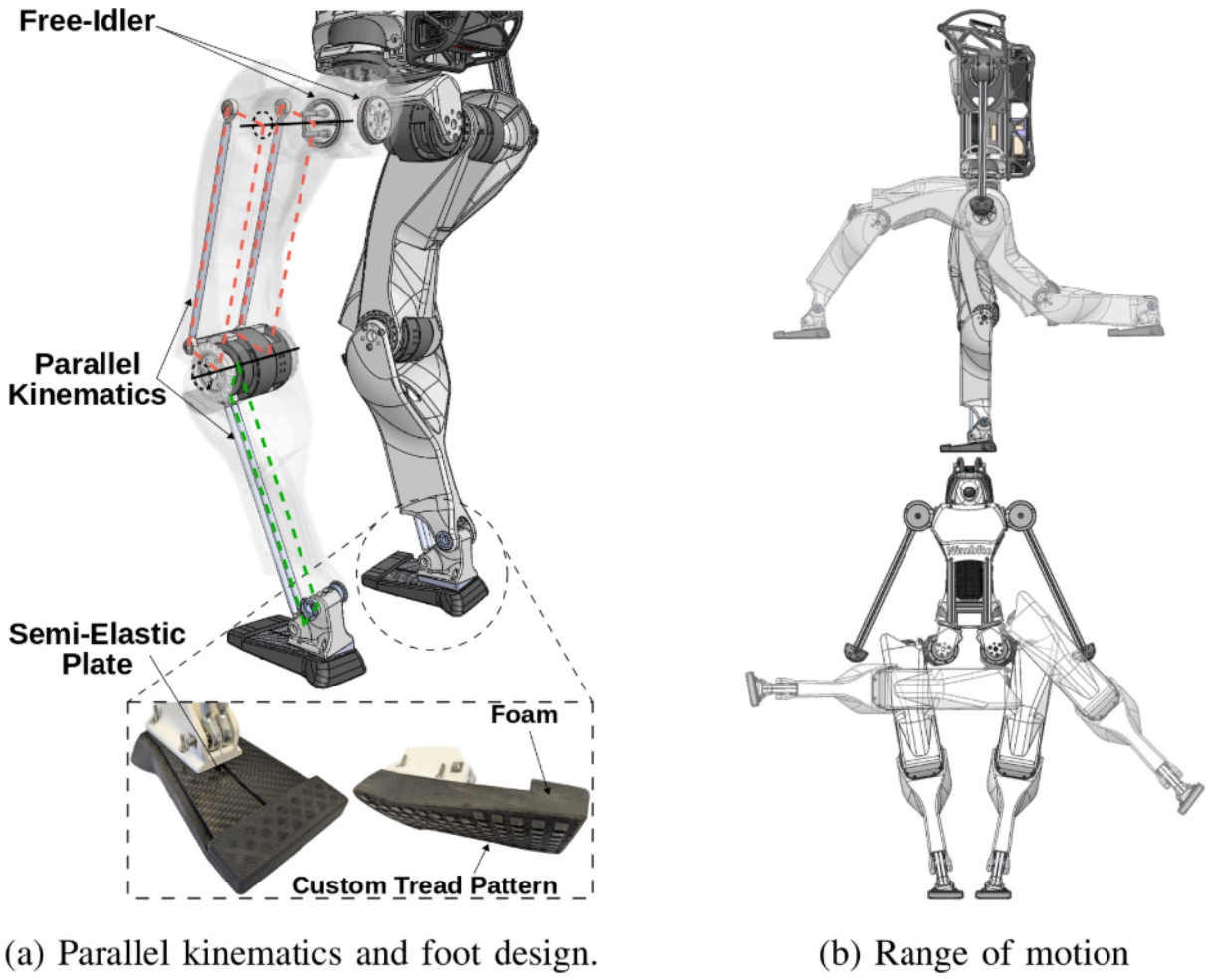

(a) Parallel kinematics and foot design. (b) Range of motion

Figure 2: Leg design details.

As almost the complete leg is 3D-printed, achieving rigidity without significant weight poses a challenge. Although CNC-milled structural components are not usually burdened with these issues, they come at a higher cost and require a production process that is more demanding in expertise, effort and costs. We reinforce the structure through modulating thickness, ribbing, and strategic use of fasteners. **AGILOped**, was prototyped and operated successfully using parts made with Polylactide (PLA), however we recommend using Nylon instead due to its durability and heat resistive properties. This approach is experimentally proven to not hinder the long-term structural integrity, as our Nylon-printed NimbRo-OP2(X) *(@ficht2017nop2, Ficht et al., 2020)* robots have operated for several years in tough RoboCup conditions without breaking any of the structural parts since their construction *(Pavlichenko et al., 2023)*. As the actuators lack a free-idler on the opposite end of the actuation axis, we implemented compact idlers mimicking the driving side of the actuator. The connection between the hip roll and pitch actuator mounts uses three screws, which simultaneously reinforce the structure and lock the hip idler bearing in place. We close the parallel kinematic chains with manually-threaded aluminum rods, with screwed-in universal joints. They are doubled and symmetrically spaced for improved axis definition, uniform loading, and redundancy, greatly enhancing the resistance to buckling and deformations.

Preprint | https://doi.org/10.64560/65530516

Bipeds with 4-DoF legs typically have point-feet, which makes them statically unstable. They need to rely on dynamic stability to maintain balance *(Ghansah et al., 2024)*. Our implementation not only decreases inertia, but allows us to use an elongated foot to achieve static stability while standing. The parallel kinematic ankle pitch joint poses a challenge, as it requires the foot to have a certain level of adaptability to the ground while simultaneously being sufficiently rigid to support the robot. The implemented design draws inspiration from biology *(Fründ et al., 2022)* and the world of sports *(Ortega et al., 2021)*. Elastic plates are angled and directly connected to the ankle to provide the foot with longitudinal stiffness and energy storage capabilities. By separating the plates, we mimic the medial and lateral arches, achieving lateral compliance. The plates are inserted into a sole, which is 3D-printed using a unique Thermoplastic Polyurethane (varioShore TPU) *(Iacob et al., 2023)* with a foaming agent. The material behaves like an elastomer below a threshold value of the printing temperature. Passing it however, makes it foam and lowers the shore hardness. The final foot design is sufficiently rigid, compliant and comes with an embedded tread pattern for increased contact friction.

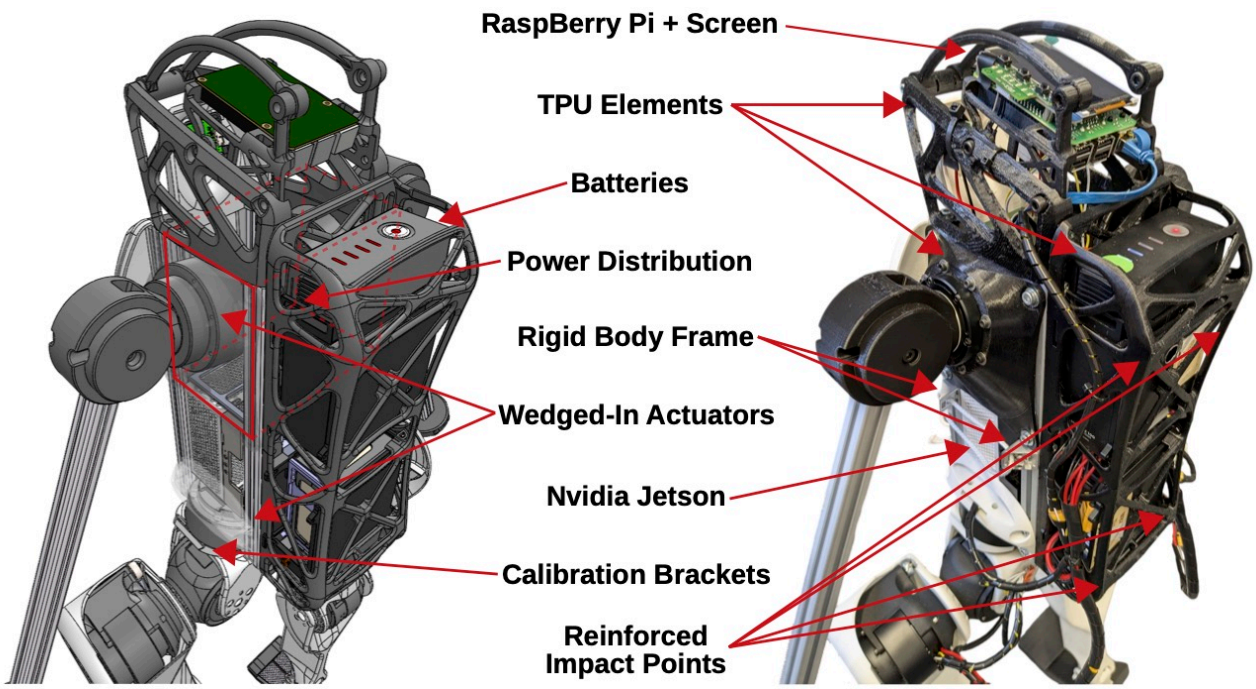

Figure 3: Upper body design details. Featuring a rigid cage, elastomer-based impact mitigation, embedded computers, batteries, and power distribution.

In total, the movable part of the leg (excluding the hip yaw within the torso) weighs 3.51kg, with actuators totaling 1.77kg. The collocated structure greatly simplifies the mechanical design without negatively impacting the inertia, as all actuators but the knee actuator are tightly packed within the hip. Furthermore, platforms which do possess ankle actuators *(@liao2024berkeley, Zhu, 2023)*, place them below the knee with a similar contribution to the reflected inertia. The lower part of the leg, comprised of the shank, ankle, foot and parallel rods sums up to 0.56kg, leaving 84% of the weight next to the hip. In the most extended configuration, the leg center of mass is only 0.16m away from the origin of the hip, which translates to 25.8% of the leg length (See Figure 1). Such

Preprint | https://doi.org/10.64560/65530516

characteristics with low rotational inertia should favor high-bandwidth control, as well as being beneficial for controllers relying on reduced-order models.

3.3 Upper Body Design

The upper body is comprised of the torso and two 1-DoF arms. The frame of the torso is built from aluminum extrusions arranged to form a cage, providing the majority of the rigidity. The actuators snugly fit between the extrusions, and lock into place through 3D-printed brackets. Given the rigidity of the aluminum frame, a plastic bracket is sufficient to support the mounting of the hips and maintain leg rigidity. Additionally, the hips have an alignment bracket, which allow the legs to collapse into a defined position for calibration. Robots prioritizing locomotion research do not necessarily need to incorporate arms. The basic arms are expected to aid **AGILOped**, in surviving falls and performing get-up motions, which provides a level of functionality above the platforms that do not have them altogether *(@liao2024berkeley, Xia et al., 2024)*. Furthermore, with **AGILOped**'s open-source nature we aim for users to refine and adapt the arm design for specific tasks. To increase impact resistance without deteriorating the performance, we employ selective compliance around the rigid frame. For this reason, the shoulder mounts are printed using TPU. This provides the shoulder with sufficient lateral compliance to mitigate falls while allowing rigid actuation in the pitch axis. The torso cage also features a *backpack* comprised of two symmetric battery compartments. Each of these is made from an off-the-shelf aluminum housing, press fit into a 3D-printed TPU enclosure. Strategic enforcing contact points and placement of supporting struts enhanced the elasticity in dispersing impact energy, already proving itself useful when working on **AGILOped**'s development.

The frame also has ample space to house the computing, sensing units, and power distribution. A Raspberry Pi with a screen is used for basic system control and mounted at the top of the robot for visual feedback. This unit, along with an optional camera form a simple robot *head*. They are protected with a 3D-printed TPU cage. Inside the torso, there is space for the power distribution and an optional NVidia Jetson computing unit see Figure 3). With this, we aim for **AGILOped**, to support modern (learning-based and model-based) control approaches and cater to a wide range of users.

4 Control Architecture

Preprint | https://doi.org/10.64560/65530516

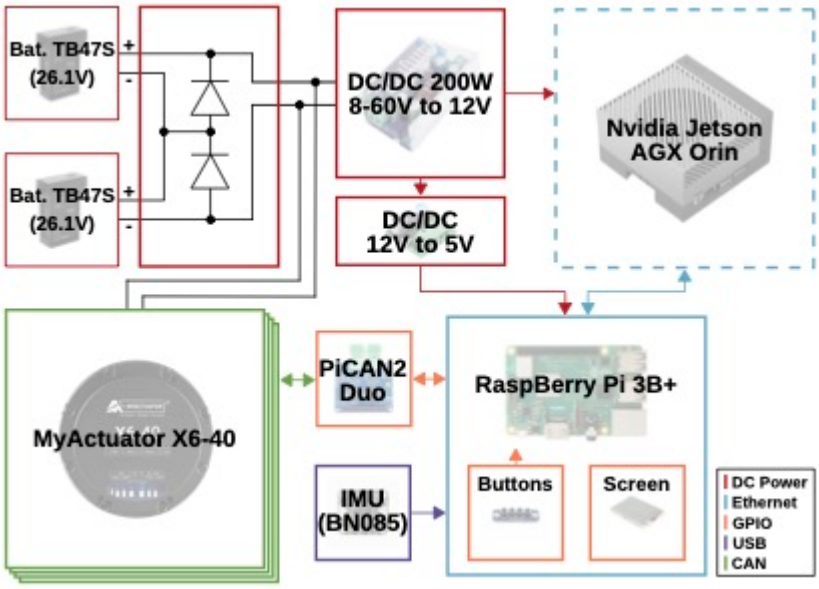

Figure 4: Electronics layout. **AGILOped**~is powered by two 26V batteries, providing a combined peak voltage of 52V to the motors. A wide-input DC/DC converter steps down the voltage to 12V for the Jetson AGX Orin. Voltage is further converted into 5V for the Raspberry Pi, serving as the base controller and CAN bus master. For higher-requirement applications, the Jetson AGX Orin can connect to the Raspberry Pi via Ethernet.

At the core of our control scheme lies a Raspberry Pi 3B+ Single Board Computer (SBC), which we chose due to its versatility, community-driven software, and long-term manufacturing support. It's form factor and compatibility allow for effortless upgrades to e.g. the more recent Raspberry Pi 5. A multitude of add-on boards *hats* exist that greatly enhance its capabilities. **AGILOped**'s setup (see Figure 4) extends the SBC with a screen for user feedback, buttons for basic controls and a PiCAN2 Duo hat to enable actuator communication over two separate CAN buses.

An Inertial Measurement Unit (IMU) is essential in giving the robot a sense of spatial motion.By fusing the 3D measurements of an accelerometer, gyroscope and magnetometer, an Attitude and Heading Reference System (AHRS) allows for precise orientation feedback. Due to the required knowledge in sensor calibration, implementation and tuning of fusion algorithms, obtaining a low-latency and precise estimate proves to be a challenge. Current dynamically capable systems have to rely on solutions in the 1000USD price range*(@katz2019mini, Zhu, 2023)*. For **AGILOped**, we have developed a plug-and-play, low-cost AHRS solution, based on RP2040 microcontroller and BNO085 AHRS modules. The BNO085 has built-in sensor calibration and fusion algorithms and various modes of output, providing the user directly with quality orientation feedback with rates up to 1kHz. To further ease the usage, we implemented USB communication through the *rosserial* library, which de/serializes ROS messages and provides straightforward ROS integration. Our open-source implementation has a total cost of 30USD and is available online. In combination with the kinematic model and joint measurements, we obtain accurate estimates of the system dynamics*(Ficht & Behnke, 2023)*.

Preprint | https://doi.org/10.64560/65530516

4.1 Low-Level Control

The Raspberry Pi operates using Ubuntu Mate OS, with ROS support and serves as the low-level controller, which we refer to as *RosPi* controller. Two CAN buses manage communication with five motors each, with a baud-rate limiting the communication to 4kHz, resulting in a maximum rate of 800Hz per motor. Due to the high frequency of communications and low-latency (measured at 1.7ms), we treat the motors as torque sources.

To enable compatibility with our position-control-based framework, impedance controllers are implemented. The target torque τ is computed from position q and velocity $\dot{q}$ errors and their associated stiffness K_P and damping K_D gains, added to a feedforward term τ_{ff} and limited to a maximum allowable value τ_{max}:

$$\tau = min(K_P(q_{set} - q) + K_D(\dot{q}_{set} - \dot{q}) + \tau_{ff}, \tau_{max}). \quad (3)$$

As the motors have absolute position encoders only on the motor shaft, the output position of the joint needs to be inferred. This is done by placing the robot into a pre-defined calibration pose, achieved by making the robot collapse his legs and resting the thighs on the hip brackets (see Figure 3).

Several software safety mechanisms have been implemented to protect both the robot and its surroundings. If a motor loses connection for more than 100ms, its internal controller will stop it. Additionally, if communications to the higher-layer node is lost, a shutdown command is sent to the motors. We have also implemented continuous monitoring of motor temperatures and voltages, their values on the Raspberry Pi screen. Persistent high temperatures, over-voltage, or torques exceeding typical values trigger warnings and shutdown the motors to prevent damage.

4.2 Higher-Level Control

AGILOped's higher-level controls are built on our open-source, ROS-based software stack that leverages the modularity of ROS. First introduced in 2013, the framework has undergone continuous improvements while maintaining its core structure. The main strength being modularity, allowing the integration of custom hardware architectures, gaits, and motion controllers through plug-ins. Motion sequences can be easily designed using keyframes through the built-in trajectory editor. This design also enables seamless integration with simulators like Gazebo and MuJoCo. The software stack has proven its versatility and adaptability across various platforms, including the Igus Humanoid Open Platform *(Allgeuer et al., 2016)*, the NimbRo-OP2X *(Ficht et al., 2020)*, and now **AGILOped**.

Preprint | https://doi.org/10.64560/65530516

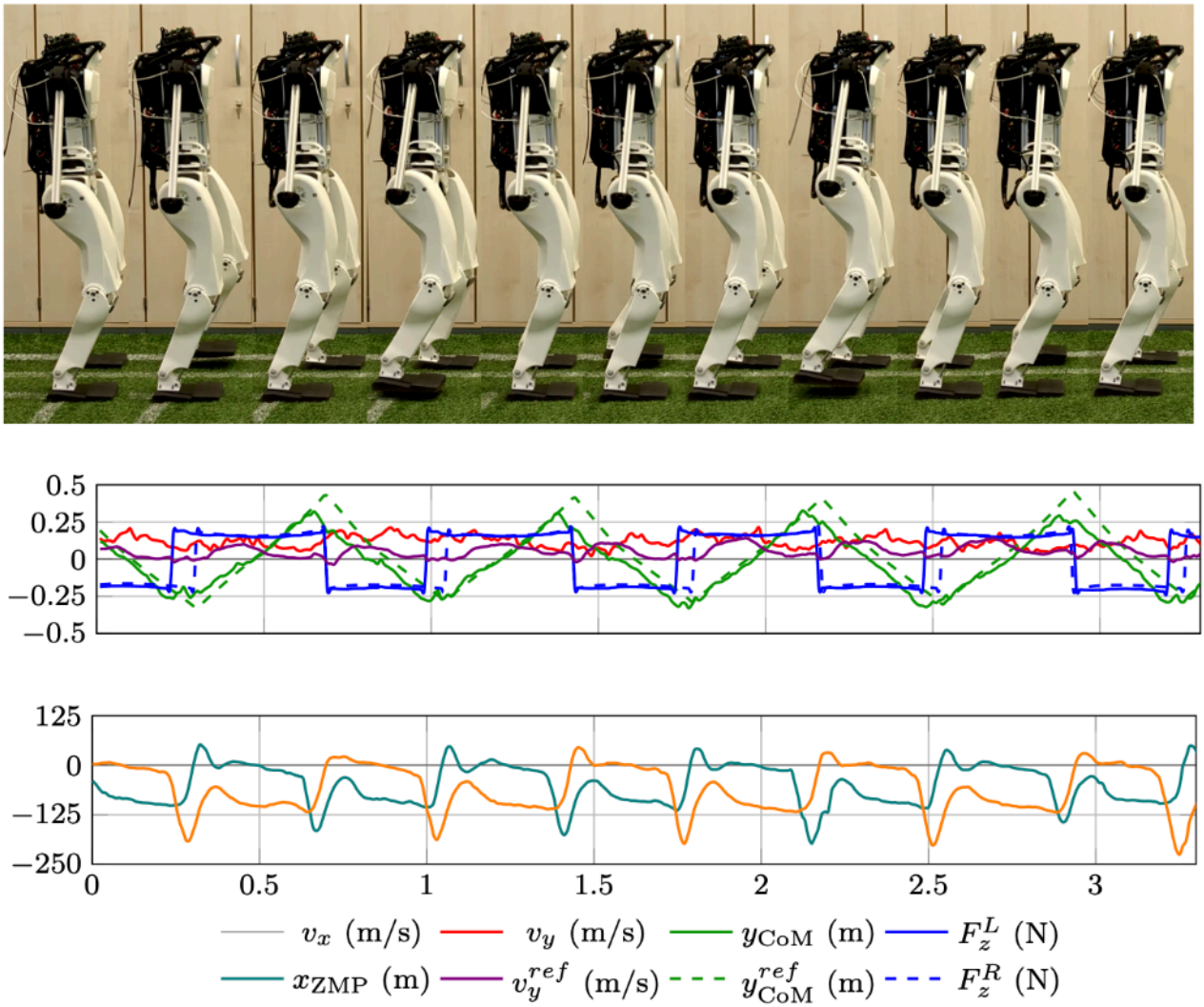

Figure 5: Forward balanced walking with an omnidirectional, feedback-enhanced, CPG-based gait. (top) motion sequence. (bottom) CoM and ZMP series, and noticeable contact force exchanges between the feet.

5 Evaluation

5.1 Bipedal Walking

Bipedal locomotion is one of the most fundamental skills for humanoid robots. For the experiments, we initially adapted and tuned the feedback-enhanced Central Pattern Generated~(CPG) gait used on the NimbRo-OP2X *(Pavlichenko et al., 2023)*. The robot is tasked with walking forward on a compliant artificial grass surface. In the lateral plane, the robot compares its current and reference Linear Inverted Pendulum~(LIP) Center of Mass~(CoM) position and velocity states *(Kajita & Tani, 1991)*. By using closed-form predictions of the end-of-step state, the gait frequency is adjusted to either delay or accelerate a step. Sagittally, a regulator that computes a desired CoM velocity from ZMP and CoM tracking errors, steers the CoM towards stability. The tracking performance, along with a time series of the gait can be observed in Figure 5. One noteworthy feature is the inclusion

Preprint | https://doi.org/10.64560/65530516

of contact forces obtained directly from joint torques and limb Jacobian, showcasing the proprioceptive capabilities of the actuators.

5.2 Jumping

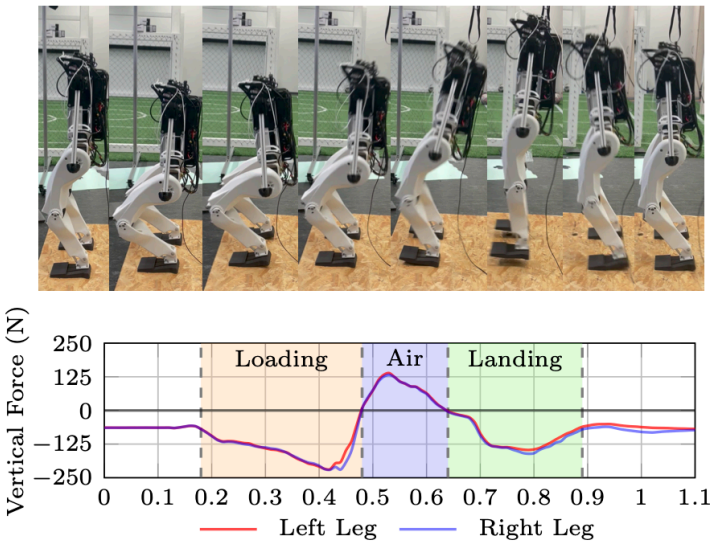

Figure 6: Vertical jump experiment. (top) Sequence of keyframes that propel the center of mass upwards and perform the landing. (bottom) Contact forces estimated using torque measurements and Jacobian.

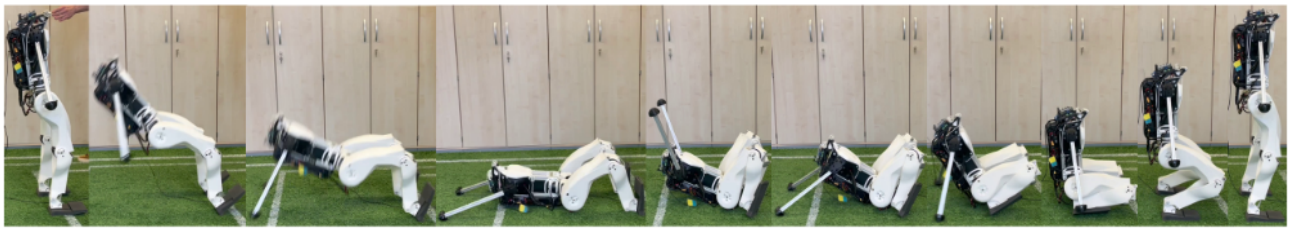

Figure 7: Time series of **AGILOped**, falling backwards and standing up again. Upon detecting the fall, the robot rapidly moves its arms backward to reduce the impact. From a prone position, it pushes itself back up onto its feet, followed by a standing-up motion.

By simply designing a set of whole-body position keyframes, we are able to swiftly move the center of mass and propel the robot upwards, as shown in Figure 6. The motions are not optimal, and merely serve as a means to display the peak power capabilities of the actuators. Without a dedicated force controller, we are unable to meaningfully apply full torque. Hence, we can reliably achieve jumps of only about 10cm. Most likely due to incorrect CoM assumptions, **AGILOped**, jumps slightly backwards, wasting some of the propelling force.

5.3 Falling Mitigation and Standing-up

To test the robustness of the hardware with respect to impacts, we intentionally push the robot from any side causing it to fall, as illustrated in Figure 7. When a fall is detected, **AGILOped**, responds by swiftly moving its arms and bracing for impact. The stiffness of the impedance controllers is greatly reduced, while damping is kept at a noticeable level. This significantly breaks the fall, allowing the robot to gently bounce off on the elastic battery backpack.

Following the fall, **AGILOped**, immediately initiates the get-up routine by retracting its legs and performing a strong push-off. This propels it back onto the feet from which getting up is straightforward, demonstrating the combined effect of the achieved actuator and structural compliance.

6 Conclusion

In this work, we have presented the hardware and software design of our humanoid robot **AGILOped**. The combination of off-the-shelf backdrivable proprioceptive actuators with high power density, standard electronics, and effective material usage within a light-weight and minimalistic design has led to the creation of a capable and affordable research platform. The mechanical and electrical simplicity make **AGILOped** accessible for novices and experts alike.

We reported experiments on walking, jumping, falling mitigation, and getting-up. We hope that other researchers will notice the potential of **AGILOped**. Its open hard- and software will enable them to contribute their developments. We envision **AGILOped** to perform robust agile locomotion together with dynamic whole-body motions like kicking.

References

Allgeuer, P., Farazi, H., Ficht, G., Schreiber, M., & Behnke, S. (2016). The igus Humanoid Open Platform: A child-sized 3D printed open-source robot for research. *KI-Künstliche Intelligenz*, *30*, 315–319.

Belli, A., Kyröläinen, H., & Komi, P. (2002). Moment and power of lower limb joints in running. *International Journal of Sports Medicine*, *23*(02), 136–141.

Booster Robotics. (2024). *Booster T1*. https://www.boosterobotics.com/

Boston Dynamics. (2017, November). *What's new, Atlas?* https://www.youtube.com/watch?v=fRj34o4hN4I

Ficht, G., & Behnke, S. (2023). Centroidal State Estimation and Control for Hardware-constrained Humanoid Robots. *IEEE-RAS International Conference on Humanoid Robots (Humanoids)*, 1–8.

Ficht, G., Farazi, H., Rodriguez, D., Pavlichenko, D., Allgeuer, P., Brandenburger, A., & Behnke, S. (2020). Nimbro-OP2X: affordable adult-sized 3D-printed open-source humanoid robot for research. *International Journal of Humanoid Robotics*, *17*(05), 2050021.

Fourier Intelligence. (2024). *Fourier GR-1*. https://fourierintelligence.com/gr1/

Fründ, K., Shu, A. L., Loeffl, F. C., & Ott, C. (2022). A Guideline for Humanoid Leg Design with Oblique Axes for Bipedal Locomotion. *IEEE-RAS International Conference on Humanoid Robots (Humanoids)*, 60–66.

Ghansah, A. B., Kim, J., Li, K., & Ames, A. D. (2024). Dynamic Walking on Highly Underactuated Point Foot Humanoids: Closing the Loop between HZD and HLIP. *arXiv Preprint arXiv:2406.13115*.

Ha, I., Tamura, Y., Asama, H., Han, J., & Hong, D. (2011). Development of Open Humanoid Platform DARwIn-OP. *SICE Annual Conf.*

Hubicki, C., Grimes, J., Jones, M., Renjewski, D., Badri-Spröwitz, A., Abate, A., & Hurst, J. (2016). ATRIAS: Design and validation of a tether-free 3D-capable spring-mass bipedal robot. *The International Journal of Robotics Research (IJRR)*, *35*. https://doi.org/10.1177/0278364916648388

Iacob, M. C., Popescu, D., & Baciu, F. (2023). Effect of process parameters on the hardness of 3D-printed thermoplastic polyurethane that includes foaming agent. *Materiale Plastice*, *60*(4), 144–154.

Kajita, S., & Tani, K. (1991). Study of dynamic biped locomotion on rugged terrain-derivation and application of the linear inverted pendulum mode. *IEEE International Conference on Robotics and Automation (ICRA)*, 1405–1406.

Kakiuchi, Y., Kamon, M., Shimomura, N., Yukizaki, S., Takasugi, N., Nozawa, S., Okada, K., & Inaba, M. (2017). Development of life-sized humanoid robot platform with robustness for falling down, long time working and error occurrence. *IEEE/RSJ International Conference on Intelligent Robots and Systems (IROS)*, 689–696. https://doi.org/10.1109/IROS.2017.8202226

Katz, B., Di Carlo, J., & Kim, S. (2019). Mini cheetah: A platform for pushing the limits of dynamic quadruped control. *IEEE International Conference on Robotics and Automation (ICRA)*, 6295–6301.

Li, J., Ma, J., Kolt, O., Shah, M., & Nguyen, Q. (2023). Dynamic Loco-manipulation on HECTOR: Humanoid for Enhanced ConTrol and Open-source Research. *arXiv Preprint arXiv:2312.11868*.

Liao, Q., Zhang, B., Huang, X., Huang, X., Li, Z., & Sreenath, K. (2024). Berkeley Humanoid: A Research Platform for Learning-based Control. *arXiv Preprint arXiv:2407.21781*.

MyActuator. (2024). *RMD-X Product Page*. https://www.myactuator.com/rmd-xplanetary-motor-1

Negrello, F., Garabini, M., Catalano, M. G., Malzahn, J., Caldwell, D. G., Bicchi, A., & Tsagarakis, N. G. (2015). A modular compliant actuator for emerging high performance and fall-resilient humanoids. *IEEE-RAS 15th International Conference on Humanoid Robots (Humanoids)*, 414–420.

Ortega, J. A., Healey, L. A., Swinnen, W., & Hoogkamer, W. (2021). Energetics and biomechanics of running footwear with increased longitudinal bending stiffness: a narrative review. *Sports Medicine*, *51*(5), 873–894.

Pavlichenko, D., Ficht, G., Villar-Corrales, A., Denninger, L., Brocker, J., Sinen, T., Schreiber, M., & Behnke, S. (2023). RoboCup 2023 Humanoid AdultSize Winner NimbRo: NimbRoNet3 Visual Perception and Responsive Gait with Waveform In-Walk Kicks. In *RoboCup 2023: Robot World Cup XXVI* (pp. 337–349). Springer.

Playter, R. R., & Raibert, M. H. (1992). Control of a biped somersault in 3d. *Proceedings of the IEEE/RSJ International Conference on Intelligent Robots and Systems*, *1*, 582–589.

SaLoutos, A., Stanger-Joncs, E., Ding, Y., Chignoli, M., & Kim, S. (2023). Design and development of the MIT humanoid: A dynamic and robust research platform. *IEEE-RAS International Conference on Humanoid Robots (Humanoids)*, 1–8.

Tardieu, C. (2010). Development of the human hind limb and its importance for the evolution of bipedalism. *Evolutionary Anthropology: Issues, News, and Reviews*, *19*(5), 174–186.

Unitree Robotics. (2024). *Unitree G1*. https://www.unitree.com/

Wilken, T., Missura, M., & Behnke, S. (2009). Designing falling motions for a humanoid soccer goalie. *4th Workshop on Humanoid Soccer Robots, International Conference on Humanoid Robots (Humanoids)*.

Xia, B., Li, B., Lee, J., Scutari, M., & Chen, B. (2024). The duke humanoid: Design and control for energy efficient bipedal locomotion using passive dynamics. *arXiv Preprint arXiv:2409.19795*.

Zhu, T. (2023). *Design of a Highly Dynamic Humanoid Robot*. UCLA Electronic Theses and Dissertations.